RSC Advances

ROYAL SOCIETY OF CHEMISTRY

www.rsc.org/advances

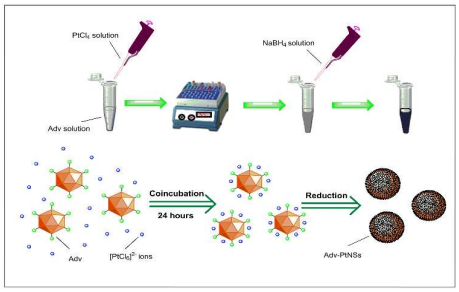

Highly biocompatible and monodisperse platinum nanoshells with diameters of ~100 nm were fabricated using adenovirus as sacrificial templates.

Self-assembly of adenovirus-templated platinum nanoshells and evaluation of their biocompatibilities

Weili Xue, Yanji Li, Jing Zhou, Zi Wang, Yanping Liu, Xuwu Zhang, Zhiwei Liu, Faming Gao*, Dawei Gao*

Applying Chemistry Key Lab of Hebei Province, Yanshan University, No.438 Hebei Street, Qinhuangdao, 066004, China.

Tel: +86 335 8387553;

Fax: +86 335 8061569

Correspondence should be addressed to Dawei Gao; dwgao@ysu.edu.cn and Faming Gao; fmgao@ysu.edu.cn

Weili Xue, Yanji Li and Jing Zhou have same contribution for the paper.

Self-assembly of adenovirus-templated platinum nanoshells and evaluation of their biocompatibilities

Abstract In this study, the self-assembly of platinum nanoshells (PtNSs) in facile conditions, using the adenovirus shuttle vector-GFP (Adv) as a biotemplate, was achieved. This novel and simple biotemplating method can be summarized as direct co-incubation of the template Adv and $PtCl_4$ solution, and then followed by the reduction of the co-incubation solution using $NaBH_4$. The prepared Adv-PtNSs were then carried out on TEM, XRD and FTIR characterization. The TEM results indicated that Adv-PtNSs, with good morphologies and monodispersity, can be obtained by controlling the concentration of $PtCl_4$ as 7.5 mM, and the obtained Adv-PtNSs were about 100 nm. The results of XRD and FITR demonstrated that the prepared Adv-PtNSs were in face-centered cubic structure, and the combination between the Adv and platinum complex ions mainly depended on –NH groups. In addition, the biocompatibilities of the prepared Adv-PtNSs to H9c2 cells were investigated. MTT assay results showed that as-prepared Adv-PtNSs had relatively high biocompatibilities, almost had no harm to H9c2 cells. Therefore, Adv-PtNSs have great potentials as bioelectrode materials for monitoring the states of organisms.

Introduction

Nowadays, nanomaterials have infiltrated into biosensors, drug carriers, disease diagnosis, cancer treatment and other aspects of biomedical technology.[1-3] There are a variety of methods for preparing nanomaterials, mainly comprising high-energy ball milling method, electrochemical method, sol-gel method and crystal template method.[4-8] However, these methods are accompanied with lots of undesired aspects, such as high cost, intractable preparation process and environmental contamination. In contrast, the biotemplate synthesis method is considered as the ideal way to prepare the nanomaterials as well as the nanoarrays, because of the advantages of precisely controllable morphology and a wide range of templated materials.[9]

Biological materials are generally selected as the templates because of wide material sources, diversified morphologies, renewability and harmlessness to organisms.[10] Up to now, there are plenty of biological materials widely studied as the templates, such as DNA, protein, virus and peptides.[11-14] Adenovirus shuttle vector-GFP (Adv) is formed on the basis of adenoviral DNA transformation and carrying green fluorescent protein (GFP) gene. Due to the unique optical signal transduction mechanism, its green fluorescent protein is suitable for serving as the optical sensors in *vivo* of living cells.[15] In addition, it has been reported that the biochemical dynamics of living cells can be measured by a GFP-dependent biosensor.[16] Furthermore, Adv is a very mature gene carrier, which has been used in clinic without toxicity.[17] On the one hand, adenovirus can tolerate the solutions of pH 3-5, so Adv can ensure the stability of three dimensional structures, and it is not affected by metal solution. On the other hand, it does not have the envelope so that the amino acid residues on the capsid can be exposed in solutions, which is beneficial for Adv to combine with Pt complex ions. Therefore, Adenovirus, a double-stranded DNA containing, and non-enveloped virus with a diameter of about 70-90 nm, is the ideal three dimensional templates, which possesses the icosahedral symmetry structures.[18]

In general, the cell activity and biological function are explored through the microscopes and biological technology test.[19] If the electrochemical technology is considered to monitor the cell growth condition and the toxicity of chemical drugs, the preparation of stable biological electrodes, with small volume, high sensitivity, high electric catalytic properties and high biocompatibility, will become the key chanllenge.[20] Platinum nanoparticles (PtNPs) have the high catalytic activities and special electrical properties, and the PtNPs, being considered as the electrode materials, have attracting wide attentions of many researchers.[21] In addition, PtNPs are chemically stable and less susceptible to corrosion of biological solution. All of

the advantages of PtNPs promote it to become the ideal choice in the area of biological electrode materials. However, among the numerous nanostructures of platinum materials, the nano-spherical shell has more excellent performances in relative to the aggregation or dispersion of the nano metal, which makes it has higher sensitivity in electrochemical applications.[22]

In this study, we introduce a peaceable and environmentally friendly route to in situ preparation of PtNSs using adenovirus as a biotemplate at room temperature. To our best knowledge, it is the first time to prepare PtNSs with uniform sizes and monodispersity. It is necessary that the biocompatibility should be tested before the PtNSs is used for the application of biological electrodes and the detecting of toxicity of drugs. At the same times, this study will provide reference values for researchers on the preparation methods and mechanism in the systems using the adenovirus as templates.

Materials and methods

Materials

$PtCl_4$ was purchased from Shanghai Jiuyue Chemical Industry Co., Ltd. Sodium borohydride ($NaBH_4$, 99%) and trypsins were purchased from Sigma. Hydrogen chloride (HCl, 36-38%) and absolute ethyl alcohol (CH_3CH_2OH) were purchased from Tianjin Kemiou Chemical Reagent Co., Ltd. The cell culture mediums (DMEM) were purchased from Gibico. MTT was purchased from Shanghai beyotime biological technology Co., Ltd. The rat cardiomyocyte cells, the 293 cells and the adenovirus shuttle vector-GFP were obtained from the Peking Union Medical College Cell Resource Center.

Preparation of Adv-PtNSs

Preparation of the adenovirus suspensions After serially periodic subcultivation, the 293 cells reached to the required concentration for the amplification of adenovirus. Afterwards, the adenoviruses with appropriate titers were added into the Petri dishes, which mixed with appropriate DMEM containing 2% fetal bovine serum. Until the 293 cells transformed to round shapes, but without detachment, the cells suspensions were collected into the centrifuge tubes and carried out repeated freezing-thawing for 3-5 times. Ultimately, the cells were completely cracked to release adenoviruses, which were then diluted and gradually centrifuged, afterwards, the precipitation was discarded, and the relatively pure virus suspension was obtained and saved in refrigerators. In order to remove the small molecular protein impurities, adenovirus solutions were then purified through dialysis treatment with the dialysis bags (D21 mm, 12000-14000 MWCO). Eventually, the pure virus solutions were obtained and saved at -80 ^oC so as to be used subsequently.

Fabrication of Adv-PtNSs *via* biotemplating 100 μL of $PtCl_4$ solution at different concentrations (2.5, 5.0, 7.5 mM) were mixed with 100 μL Adv suspensions (1.1×10^{11} VP/mL) respectively, and then the mixtures were incubated in a shaking bath on conditions of avoiding light for 24 h, 130 rpm, 15 ^oC. After that, the freshly prepared $NaBH_4$ solution (5 mM) was added into the mixtures until the incubated liquid turned ash-black, indicating that $[PtCl_6]^{2-}$ was reduced to Pt^0, and thus the Adv-PtNSs solution was obtained. For comparison, 100 μL monodisperse platinum nanoparticles solution (5.0 mM) which was prepared by the reaction of $PtCl_4$ and sodium borohydride ($NaBH_4$), was mixed with the isovolumetric Adv suspensions, acting as the control group.[23]

Characterization of Adv-PtNSs

In order to analyze the morphologies of prepared Adv-PtNSs, TEM images of Adv-PtNSs was observed. Furthermore, the Adv suspension was negative-stained by the 2 % (W/V), pH 7.0 fresh phosphotungstic acid dye solution, which was designed as the control group. Energy-dispersive X-ray (EDX) analysis was obtained with an EDAX detector installed on the same TEM. Malvern Zetasizer ZS (Malvern Instruments, UK) was used to measure the sizes and surface zeta potentials of the prepared Adv-PtNSs. The mean diameters and zeta potentials of the Adv-PtNSs were determined by dynamic light scattering (DLS) and electrophoretic mobility measurements, respectively. The zeta potential of an Adv solution was also measured. All

measurements were repeated three times at 25 °C. The platinum nanoshells were tested by Fourier transform infrared spectroscopy (FTIR) for investigating the formation mechanism on the aspects of chemical bonds, and the adenovirus suspensions were also detected for contrast. In addition, the prepared Adv-PtNSs were tested through the X-ray diffraction (XRD) so as to determinate the crystal types of platinum in the complexes.

Biocompatible evaluation of Adv-PtNSs

The life activities and function of organisms are based on the fundamental structures of cells. Therefore, the common biological toxicities of nanomaterials derive from the destruction on cells' structures. In order to develop the biological electrodes without cytotoxicities, the Adv was used as the templates for synthesizing Adv-PtNSs with particular morphologies, and the biocompatibility was evaluated for determining its potential ability as biological electrodes. Therefore, the classical MTT assay was utilized to analyze the biocompatibilities of Adv-PtNSs to H9c2 cells in *vitro*.

H9c2 cells in the logarithmic phase were inoculated into 96-well plates containing 0.1 mL of complete culture medium in each well, and allowed to attach for 24 h. Adv-PtNSs that possessed the brilliant morphology, whose initial concentration was diluted to 0.25 mM and followed by the respective dilution ratio of 1, 10^{-1}, 10^{-2}, 10^{-3}, 10^{-4} and 10^{-5}, were added into 96-well plates (10 μL per well). 24 hours later, the cells mixtures were incubated with 10 μL fresh MTT solutions (5 μg/mL) for 4 hours additionally. Afterwards, the reaction liquids which turned purple, were abandoned, and the DMSO dissolving solutions (200 μL per well) were injected. The equal concentration of Adv templates and Pt nanoparticles were considered as the control groups. Blank culture fluid served as the zeroing group, and the cells suspensions with no drugs but PBS added, served as the negative control group. Eventually, the absorbance of samples was measured by an ELISA reader (MK3, Thermo Co., USA) at 595nm.

Statistical analysis

All the obtained data are expressed as mean ± standard error unless particularly outlined. Origin software (version7.0) was utilized to deal with numeric plots. SPSS statistical software (version 13.0) was performed for statistical analysis. Statistical significance was assessed by a one-way analysis of variance test. Differences were considered statistically significant if P was <0.05.

Results and discussion

Formation and characterization of the prepared Adv-PtNSs

The control groups of Adv-PtNPs and negatively stained Adv As shown in Fig 1a, the direct reaction of Adv and monodisperse PtNPs was designed as a control sample which was detected by TEM accurately. The Adv were not covered by the PtNPs as shown in the red boxes, and there were lots of monodisperse PtNPs in the background. In addition, the negatively stained Adv was served as a negative control group, and its morphology was observed by TEM (shown in Fig. 1b). The gray white balls were complete adenoviruses which were stained by phosphotungstic acid previously, and the tiny white particles were the free capsids particles that dropped down from the cracked virus.

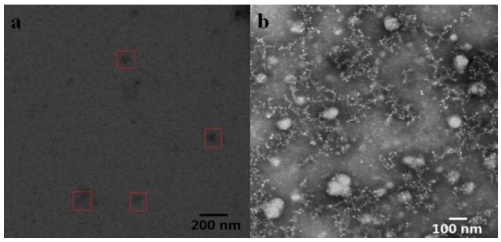

Fig. 1 TEM images of control samples: (a) Adv-PtNPs, (b) Adv.

Effect of the $PtCl_4$ concentration on the Adv-PtNSs The $PtCl_4$ solutions in different concentrations (2.5, 5.0, 7.5 mM) were mixed with Adv suspensions respectively, and the morphologies of Adv-PtNSs composites were characterized by TEM as shown in Fig 2. With the concentration of $PtCl_4$ increasing, the coverage rates of platinum nanoparticles appeared correspondingly increasing, and Adv-PtNSs exhibited the special spherical-shell structures.

Under the condition of 2.5 mM $PtCl_4$, Fig. 2a

showed that only a few of PtNPs were adsorbed on the capsid of Adv, which was ascribed to the excessively low concentration ratio of $PtCl_4$/Adv. Therefore, there were not enough platinum particles coating on the exposed surfaces of adenovirus. In Fig. 2b, when the concentration of $PtCl_4$ was 5.0 mM, plenty of black platinum nanoparticles could be discovered clearly in this composite system which emerged gray-black, and the profiles of the spherical shells were not smooth, indicating that the surfaces of Adv were not covered by the platinum nanoparticles completely. Furthermore, the diameters of Adv-PtNSs were mainly between from 60 nm to 90 nm. As shown in Fig. 2c, with the concentration increasing from 5.0 mM to 7.5 mM, Adv-PtNSs composites were blacker than before, and the average diameter was approximately 100 nm that obviously exceeded that of Adv-PtNSs prepared with 5.0 mM $PtCl_4$ because of the more absorption of PtNPs on Adv. Therefore, compared with the other two samples, the sample prepared with 7.5 mM $PtCl_4$ possessed the better morphologies.

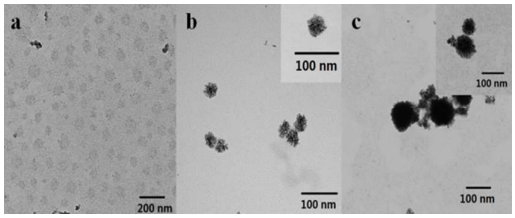

Fig.2 TEM images of Adv-PtNSs with different concentrations: (a) 2.5 mM, (b) 5.0 mM and (c) 7.5 mM

EDX analysis As shown in Fig. 3, Energy dispersive spectroscopy (EDS) was performed on a random selection of Adv-PtNSs prepared with 7.5 mM $PtCl_4$, showing that the sample was composed of Pt. The Cu signal derives from the TEM grid, and the C peak arises from the capsid proteins of Adv and the carbon-coated Cu TEM grid. The N, O, S peaks attributed to the Adv template. Consequently, it can be concluded that Pt complex ions combined with Adv to form Adv-PtNSs indeed.

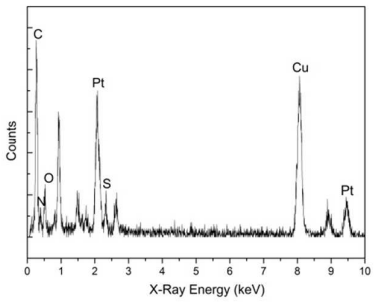

Fig.3 EDS spectrum of Adv-PtNSs

Zeta potential and particle size In this study, the zeta potentials were determined by electrophoretic mobility measurements. The surface zeta potentials of the single Adv solution and the prepared Adv-PtNSs can be seen in Fig. 4. The single Adv solution had a marked negative charge (-26 ± 1.61 mV), which was ascribed to a mass of lysine residues of capsid protein on the surface of Adv. The surface zeta potential of the prepared Adv-PtNSs was -30.3 ± 1.9 mV, less than that of pure Adv solution, which might be contributed to the fact that there was still a handful of $[PtCl_6]^{2-}$ adsorbing on the surface of Adv after reduction. Moreover, the high negative charges on the surface of the as-prepared Adv-PtNSs contributed to the stability of Adv-PtNSs in solution. The particle sizes were detected by DLS. The size distribution with the log-normal fitting curve of the prepared Adv-PtNSs is shown in Fig. 5. The average diameter of the Adv-PtNSs was around 117.12 nm, larger than 100 nm, indicating that slight aggregation of Adv-PtNSs occurred. The result also indicated that the particle sizes of the prepared AOC-PtNPs were relatively uniform.

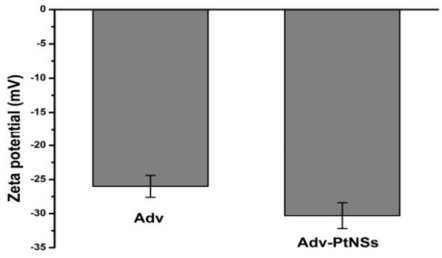

Fig.4 Surface zeta potentials of Adv and Adv-PtNSs. Data represent mean ± SE (n=3).

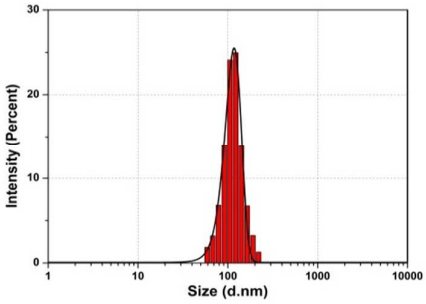

Fig.5 Size distribution of as-prepared Adv-PtNSs with the long-normal fitting curve.

Formation mechanism and crystalline structure

According to the foregoing, Adv-PtNSs prepared with 7.5 mM $PtCl_4$ had the excellent morphologies. Hence, the sample Adv-PtNSs prepared with 7.5 mM $PtCl_4$ and Adv solutions were selected to be freeze-dried into powder and carried out on FTIR characterization, and the result of FTIR was shown in Fig. 6. The capsid proteins of adenovirus were principally composed of lysine (Lys), and FTIR spectrum was mainly analyzed on amine groups, amide groups, and methylene groups. Compared with the Adv, the wavenumbers of Adv-PtNSs at 1630 cm^{-1}, 1530 cm^{-1} and 1050 cm^{-1} were decreased obviously, and these three peaks were derived from stretching vibration of N-H bonds, bending vibration of N-H bonds and stretching vibration of C-N bonds. All the changes of wavenumbers can be attributed to the fact that -N-Pt groups formed during the reaction, the amount of -NH- groups were decreased, and the vibration of surrounding C-N bonds were affected. Thus, $[PtCl_6]^{2-}$ could combine with the amino groups on the surface of Adv specifically so that the structures of the spherical shells could be formed through further reduction by $NaBH_4$.

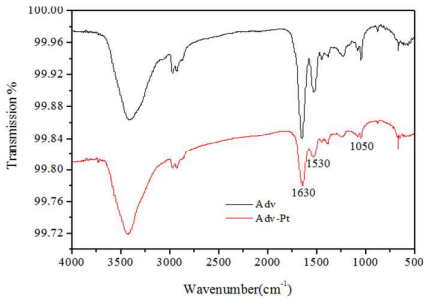

Fig. 6 FTIR spectra of Adv and Adv-PtNSs

Adv-PtNSs were carried out by the centrifugation, which were then freeze-dried into powder for XRD detection, and the results were shown in Fig. 7. The diffraction peaks (2θ: 39.67°, 46.16 °, 67.44 ° and 81.23 °) are corresponding to the crystal faces of the face-centered cubic (FCC) of platinum ((111), (200), (220), (311)), respectively, therefore, the crystal structures of PtNPs which enveloped on the capsid uniformly, were face-centered cubic structures (JCPDS Card No. 87-0646). It can be seen from fig. 7 that these four diffraction peaks of platinum crystal were relatively sharp and there were not significant impurity peaks on horizontal line, indicating the prepared Adv-PtNSs complexes possessed the high purity.

According to Fig. 7, the grain sizes of platinum nanoparticles were calculated by Scherrer function, and the results were obtained from the Scherrer formula: $D = K\gamma/B\cos\theta$ (K=0.89, γ=0.154056 nm). The grain sizes of four crystal faces ((111), (200), (220), (311)) of PtNPs on the surface of Adv were 8.73, 8.11, 9.46 and 15.94 nm, respectively. By contrast, the grain sizes of four crystal faces of PtNPs growing without Adv template were 11.14, 10.31, 8.96 and 9.26 nm, respectively. By comparing the grain sizes of PtNPs growing with Adv and PtNPs growing without Adv, significant differences could be found, which demonstrated that the grain sizes of PtNPs were closely related to its growing substrate. The mean grain size of the PtNPs on the surface of Adv was 10.56 nm, and the diameter of the Adv from Fig.1b is about 90 nm. Theoretically, the diameter of the Adv-PtNSs should be adding the diameter of Adv and double grain size of PtNPs, which was consistent with the result of Fig.5. Therefore, the TEM results of Adv, size distribution result of Adv-PtNSs and the XRD result converged to the fact that PtNPs surely coated on the surface of Adv to form Adv-PtNSs.

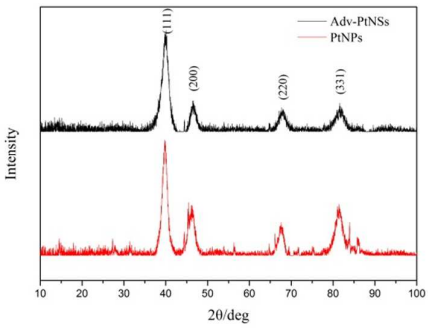

Fig. 7 XRD pattern of Adv-PtNSs (7.5 mM).

Through analyzing the preparation process of Adv-PtNSs composites and the results of TEM and FTIR, it could be discovered that platinum nanoshells could be formed after the co-incubation of Adv and $PtCl_4$ followed by reducing, and the absorption peaks of N-H bonds and C-N bonds vibration that stemmed from the capsids protein of Adv were changed. However, the directed reaction of Adv and PtNPs cannot form the nanoshells, indicating that the surfaces of Adv possessed the specific sites for combining with $[PtCl_6]^{2-}$ but not for PtNPs. This consequence was different from the cytochrome which could combine with two kinds of platinum, it might be due to the fact that the capsid proteins of Adv were mainly composed of lysines.[24] However, cytochrome contains a variety of amino acids so that it can provide more kinds of binding sites to combine with platinum.[25]

Biocompatibility assessment of Adv-PtNSs

The Pt nanoshells were investigated by MTT assay for biocompatibility assessment. Fig. 8 showed the effects of nanoshells and control drugs on the survival rates of cells. The Adv-PtNSs solutions in different concentrations had different influence on the survival of H9c2 cells, resulting in the significant difference of biocompatibility. As shown in Fig. 8, the biocompatibility of Adv-PtNSs located between PtNPs and Adv invariably in the same groups, indicating that the biocompatibility of the composite system was affected by both Adv and PtNPs. When the concentration of Adv-PtNSs exceeded 2.5×10^{-4} mM, its biocompatibility was mainly influenced by the adenovirus templates, while the concentration reduced to 2.5×10^{-5} mM, its biocompatibility was mainly influenced by PtNPs. What's more, PtNPs covered around the surface of Adv so that the biocompatibility of Adv-PtNSs was greatly affected by PtNPs. Impressively, when the concentration of the Adv-PtNSs composites was up to 2.5×10^{-1} mM, the cell viability could still reach 90.14%, which was already a very high cells survival rate. Therefore, the cytotoxicity of Adv-PtNSs even can be neglected and its biocompatibility was outstanding. The Adv-PtNSs whose concentrations ranged from 2.5×10^{-3} to 2.5×10^{-2} mM can be used as electrode materials for monitoring the growth of cells and the cytotoxicity of chemical drugs in real-time, while the monodispersed platinum nanoparticles in the same concentration cannot reach the high biocompatibility.

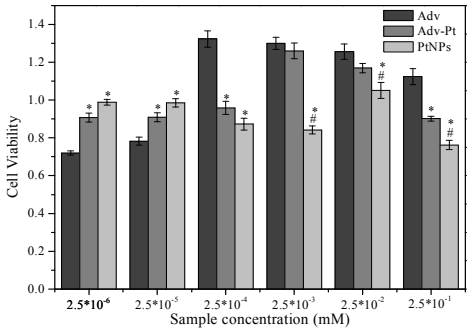

Fig. 8 Biocompatibility histogram of Adv-PtNSs and control samples with different concentrations. (* indicates that $P<$ 0.05 compared with Adv; # indicates that $P<$ 0.05 compared with Adv-Pt)

Conclusions

Adenovirus with regular icosahedron structures provided the excellent templates for the formation of platinum nanoshells, which was incubated with platinum chloride solutions followed by reduction using sodium borohydride, and ultimately the platinum nanoshells were fabricated successfully. According to the TEM results, the relatively superior morphology of platinum nanoshells (7.5 mM) with a diameter of about 100 nm was obtained. XRD and FITR demonstrated that the prepared Adv-PtNSs were in face-centered cubic structure, and the combination between the Adv and platinum complex ions mainly depended on –NH groups. According to MTT assay results, the prepared Adv-PtNSs showed high biocompatibilities to H9c2 cells. Impressively, the cell

viability can still reach 90.14%, when the concentration of prepared Adv-PtNSs was up to 2.5 $\times 10^{-1}$ mM. Therefore, the prepared Adv-PtNSs have great potentials as bioelectrode materials for monitoring the states of organisms.

Acknowledgments

This work was financially supported by a research fund from the National Natural Science Foundation (No. 21476190), Hebei Province Key Basic Research Foundation (No.15961301D) and Qinhuangdao Science and technology research and development Project (No. 201202B029).

Reference

1. A. A. Saei, J. E. N. Dolatabadi, P. Najafi-Marandi, A. Abhari and M. de la Guardia, *TrAC Trends in Analytical Chemistry*, 2013, **42**, 216-227.
2. V. Biju, *Chemical Society Reviews*, 2014, **43**, 744-764.
3. K. Park, *ACS nano*, 2013, **7**, 7442-7447.
4. F. Zhang, C. Wang and M. Zhu, *Scripta materialia*, 2003, **49**, 1123-1128.
5. A. K. Patra, A. Dutta and A. Bhaumik, *ACS applied materials & interfaces*, 2012, **4**, 5022-5028.
6. K. Matsuda, H. Yamaguchi, T. Sakano, M. Ikeda, N. Tanifuji and M. Irie, *The Journal of Physical Chemistry C*, 2008, **112**, 17005-17010.
7. M. Zhou, S. Chen, S. Zhao and H. Ma, *Chemistry Letters*, 2005, **34**, 1670-1671.
8. M. Yamamoto, Y. Kashiwagi, T. Sakata, H. Mori and M. Nakamoto, *Chemistry of materials*, 2005, **17**, 5391-5393.
9. N. Ma, E. H. Sargent and S. O. Kelley, *J. Mater. Chem.*, 2008, **18**, 954-964.
10. H.-J. Liu, X.-M. Wang, W.-J. Cui, Y.-Q. Dou, D.-Y. Zhao and Y.-Y. Xia, *Journal of Materials Chemistry*, 2010, **20**, 4223-4230.
11. Z. Wang, J. Zhang, J. M. Ekman, P. J. Kenis and Y. Lu, *Nano letters*, 2010, **10**, 1886-1891.
12. S. Goto, Y. Amano, M. Akiyama, C. Böttcher and T. Komatsu, *Langmuir*, 2013, **29**, 14293-14300.
13. C. K. Jeong, I. Kim, K.-I. Park, M. H. Oh, H. Paik, G.-T. Hwang, K. No, Y. S. Nam and K. J. Lee, *ACS nano*, 2013, **7**, 11016-11025.
14. C.-L. Chen, P. Zhang and N. L. Rosi, *Journal of the American Chemical Society*, 2008, **130**, 13555-13557.
15. A. Ibraheem and R. E. Campbell, *Current opinion in chemical biology*, 2010, **14**, 30-36.
16. M. De, S. Rana, H. Akpinar, O. R. Miranda, R. R. Arvizo, U. H. Bunz and V. M. Rotello, *Nature chemistry*, 2009, **1**, 461-465.
17. P. Wonganan and M. A. Croyle, *Viruses*, 2010, **2**, 468-502.
18. G. R. Nemerow, P. L. Stewart and V. S. Reddy, *Current opinion in virology*, 2012, **2**, 115-121.
19. E. Nyarko, T. Hara, D. J. Grab, A. Habib, Y. Kim, O. Nikolskaia, T. Fukuma and M. Tabata, *Chemico-biological interactions*, 2004, **148**, 19-25.
20. H. Ben-Yoav, A. Biran, R. Pedahzur, S. Belkin, S. Buchinger, G. Reifferscheid and Y. Shacham-Diamand, *Electrochimica Acta*, 2009, **54**, 6113-6118.
21. W. Gao, S. Sattayasamitsathit, J. Orozco and J. Wang, *Journal of the American Chemical Society*, 2011, **133**, 11862-11864.
22. S. Guo, S. Dong and E. Wang, *The Journal of Physical Chemistry C*, 2009, **113**, 5485-5492.
23. W. Xue, J. Zhou, D. Gao, F. Gao, Z. Wang, L. Luo, Y. Li and Z. Liu, *New Journal of Chemistry*, 2015, **39**, 3608-3614.
24. C. R. O'Riordan, A. Lachapelle, C. Delgado, V. Parkes, S. C. Wadsworth, A. E. Smith and G. E. Francis, *Human gene therapy*, 1999, **10**, 1349-1358.
25. A. Casini, C. Gabbiani, G. Mastrobuoni, L. Messori, G. Moneti and G. Pieraccini, *ChemMedChem*, 2006, **1**, 413-417.